

IDUNAS	NATURAL & APPLIED SCIENCES JOURNAL	2020 Vol. 3 No. 2 (34-48)
--------	---------------------------------------	------------------------------------

## RF Marker Simulation Model for Interventional MRI Applications

Research Article

Engin Baysoy<sup>1\*</sup> 

<sup>1</sup> Biomedical Engineering Department, İzmir Democracy University, İzmir, Turkey

Author E-mails

engin.baysoy@idu.edu.tr

\*Correspondance to: Engin Baysoy, Biomedical Engineering Department, İzmir Democracy University, İzmir,

Turkey

Tel: +90 0232 260 1001

DOI: 10.38061/idunas.748352

Received: 05.06.2020; Accepted: 08.07.2020

### Özet

Mevcut görüntüleme modaliteleri ile kıyaslandığında Manyetik Rezonans Görüntüleme (MRG) sisteminin sahip olduğu üstünlüklerin herkes tarafından kabul görmesiyle girişimsel kardiyovasküler ameliyatların MRG tarayıcı ile yapılması yönünde bir eğilim doğmuştur. Ancak halen güvenilir ve MRG uyumlu girişimsel aletlerin mevcut olmaması, bu klinik uygulamaların MRG rehberliğiyle yapılabilmesinin önündeki en büyük sorundur. Klinikteki kalp içi uygulamalarında MRG kullanımının yaygınlık kazanabilmesi için rehber tel ve kateterlerin ticari olarak üretiminde görüntülenebilirlik, küçültülebilirlik, esneklik ve güvenlik gibi kriterlerin dikkate alınması gerekmektedir.

Bu çalışmada, farklı şekillerde dizayn edilmiş RF işaretleyici yapılarının üretimini yapmaksızın güvenilir bir şekilde değerlendirebilmek için, konumdan bağımsız bir simülasyon modelinin uygulanabilirliği doğrulanmıştır. Model içerisinde kullanılan RF bobin tasarımları, daha önce deneysel yöntemler ile üretilmiş klinik olarak kullanılacak ve MRG uyumlu RF işaretleyiciler ile aynı ölçü ve özellikleri taşımaktadır [1]. Comsol Multiphysics programı simülasyonları ile sonlu eleman yöntemi kullanılarak, farklı RF bobin tasarımlarının elektriksel ve manyetik karakteristiği matematiksel olarak analiz edilmiştir. MRG ortamını resmeden kanıtlanmış bir benzetim ortamı, farklı RF işaretleyici prototip tasarımlarının üretimlerinin yapmaksızın, birçok açıdan birbiriyle kıyaslanmasını mümkün kılacaktır. Bu çalışmada sunulan benzetim platformu gelecekte üretilmesi planlanan yeni RF işaretleyici tasarımlarının, görünürlük, güvenilirlik, sinyal gürültü oranı, ısınma miktarı ve kalite faktörü gibi özelliklerinin belirlenmesi açısından kullanışlı bir ortam sağlamaktadır.

**Anahtar Sözcükler:** Girişimsel MRG, RF işaretleyici, MRG uyumluluk, SEM simülasyonları.

### Abstract

Compared to the other imaging modalities Magnetic Resonance Imaging (MRI) system has many advantages. There is a great demand to carry out interventional cardiovascular procedures under MRI scanner. However, the lack of visible markers and MRI compatible interventional instruments and devices,

is the main problem for realizing clinical applications with MRI guidance. In order to provide widespread usage of MRI for endovascular operations, commercial catheters and guidewires must be manufactured by considering many performance criteria including visualization, miniaturization, flexibility and safety.

In this study, an orientation independent simulation model was developed and validated to obtain a reliable method for evaluating the designed RF marker structures in a MRI environment. Utilized RF coil designs have similar size and properties with former constructed clinical grade MRI compatible RF markers in experimental works [1]. Finite Element Method (FEM) simulations were carried out for different RF coil designs to make the computational analysis of their electrical and magnetic characteristics by using COMSOL Multiphysics program.

By delineating an approved simulation platform of a MRI environment, various different designs of RF marker prototypes can be compared between each other in many aspects, instead of realizing these models. Proposed simulation platform enables a convenient facility to determine various parameters of micro coils that have significant effects on visibility and safety performance of the candidate designs including signal to noise ratio (SNR) and Quality (Q) factor, RF induced heating and specific absorption rate (SAR).

**Keywords:** Interventional MRI, MRI compatibility, RF marker, FEM simulations.

## 1. INTRODUCTION

Magnetic Resonance Imaging (MRI) guidance was intended to be a new platform by operators in order to realize catheter-based imaging and therapeutic procedures without usage of x-ray. Beside ionizing radiation free imaging modality benefits, operators favor MRI to perform complex interventional cardiovascular operations because of its accepted advantages including superior intrinsic soft tissue contrast and multi slice imaging technique [2]. Furthermore, compared to conventional x ray based modalities it is possible to collect reliable and real time physiologic cardiac parameters via MRI such as flow, volume, pressure, diffusion, perfusion, temperature, motion, and etc. [3].

Despite many promising progresses in many reports, unavailability of commercially proved MRI safe and visible instruments still makes interventional cardiovascular MRI (iCMRI) unrealistic for the treatment of cardiovascular diseases. Since MRI physical nature has a high magnetic field inside operation room, conventional interventional instruments and devices that consist of conductive materials cannot be utilized with interventional applications under MRI. Beside of MRI safety concerns with magnetic field effect and RF induced heating problems, medical devices implanted into patient body must be visible and possible for tracking while operator steering the catheter through the vessels and cardiac chambers of patient.

For semi-active and active catheter designs, in order to highlight the interventional medical devices under MRI, miniature size resonant frequency (RF) markers have to be placed over catheter shaft. Tuning of resonance frequency (RF) marker at Larmor frequency of MRI scanner, is the key for maximum interaction between RF marker and standard coil connected to MRI scanner.

Currently available RF markers in semi-active or active devices contain conventional components such as solenoid coils, nonmagnetic capacitors, diodes, and wires. However, all these rigid analog circuit components and the soldering process itself increase overall device profile and affect device mechanical properties (flexibility, endurance, and etc.) unfavorably.

An orientation independent simulation model was validated to obtain a reliable method for evaluation of the characteristics of the designed RF marker structures into the MRI platform without the need of fabrication. Finite Element Method (FEM) simulations were carried out for developed RF marker

prototype and different RF coil designs to obtain the computational analysis of their electrical and magnetic characteristics in COMSOL Multiphysics program.

Experimentally realized RF marker prototype was placed into a birdcage coil in a MRI simulation environment and its magnetic and electrical characteristics were examined in terms of electromagnetic field homogeneity and B<sub>1</sub> field circularity in the volume of interest. Adding to that performance of different RF coil designs were studied when the RF coil was positioned into different orientations with respect to the birdcage coil in virtual MRI platform.

By delineating an approved simulation platform of a MRI environment, various different designs of RF marker prototypes can be compared between each other in many aspects, instead of realizing these models. Proposed simulation platform enables a convenient facility to determine various parameters of micro coils that have significant effects on visibility and safety performance of the candidate designs including signal to noise ratio (SNR) and Quality (Q) factor, RF induced heating and specific absorption rate (SAR).

## 2. MATERIALS & METHODS

### Simulation Set Up in MRI for A Birdcage Coil

An orientation independent simulation model was constructed to evaluate the visibility performance of different RF marker designs in MRI environment. Designing a virtual platform for testing RF marker prototypes with different orientation according to standard birdcage coil helps to analyze the induced electromagnetic field, homogeneity distortion and B<sub>1</sub> field circularity in the volume of interest.

### Simulation Workflow

For setting up and solving a simulation model in Comsol Multiphysics 5.3, it is necessary to follow a standard workflow. Sequence of steps for a standard workflow was expressed below;

- Setting up a model environment
- Creating a geometry
- Specifying materials and their properties
- Defining physics and boundary conditions
- Creating a mesh
- Running simulation
- Postprocessing results

By following the regarding steps, we set up our simulation model, and evaluated the results according to our assumptions.

### Validation of Finite Element Modeling of a Birdcage Coil

RF birdcage coils have become widespread in the field of MRI imaging. Their simplicity in design followed by a high homogenous magnetic field due to continuous sinusoidal current distribution on the surface of the coil led to their popularity. Modeling the birdcage coil in a 3D simulation environment helps to examine the electromagnetic field in the volume of interest, such as field homogeneity, B<sub>1</sub> field circularity [4]. Starting point of the simulation model studied in this study was an available model in COMSOL

Multiphysics model. Finite Element Method (FEM) model of low-pass birdcage coil in order to obtain a homogenous magnetic field and circular  $B_1$  field inside the birdcage coil in 3 Tesla MRI was already prepared and shared by program supplier [5]. In our study, prepared and exist model by program supplier for 3 Tesla MRI, was modified and made suitable for 1.5 Tesla MRI scanner, given in Figure 1. Similar conditions were set up and evaluated for 1.5 Tesla MRI environment.

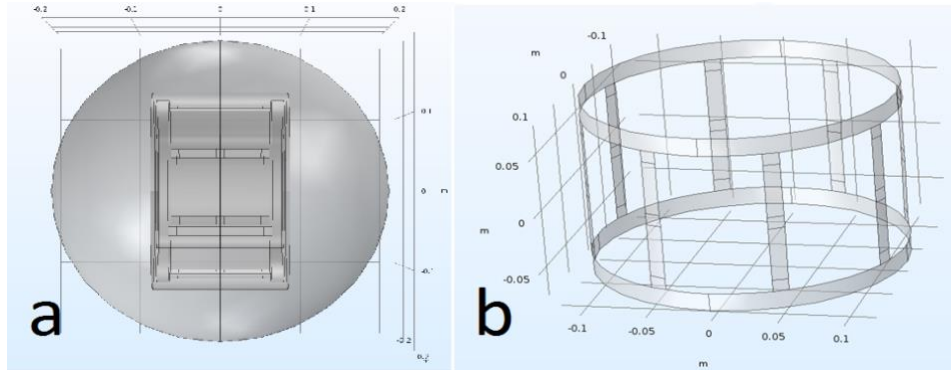


**Figure 1.** a) Geometric model of whole MRI virtual platform b) Geometric model of a low-pass birdcage coil inside MRI environment.

Geometric parameters of custom designed low-pass birdcage coil;

Radius of the sphere	: 20 cm
Radius of the birdcage coil	: 12 cm
Height of the birdcage coil	: 15 cm
Length of the capacitive elements	: 1 cm
Number of the capacitive elements	: 22
Number of the legs	: 8
Number of the activation ports	: 2

In order to validate the designed MRI platform, a phantom was placed into the middle of the model that has the similar properties with ASTM F2182 phantom (Relative permittivity: 80, relative permeability: 1, electrical conductivity: 0.47 S/m). Electric field distribution on the surface and the volume of the constructed phantom, shown in Figure 2, was compared with previously reported electric field distributions in the ASTM phantom [6].

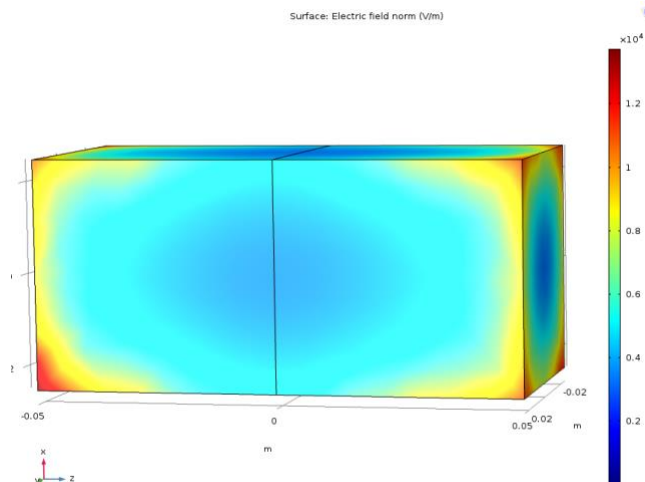


**Figure 2.** The phantom that simulates a saline water filled tank with 5 cm width, 5 cm depth and 10 cm length.

## Quadrature Excitation in Frequency Domain Analysis

First part of our simulation studies was inspired by thesis studies [4,5] that utilized program of Comsol Multiphysics while inspecting effects of varied conditions, and parameters of instruments in MRI scanner environment. According to these former studies, in order to effectively design a birdcage coil, capacitance tuning is necessary to determine optimum capacitance value to obtain homogenous magnetic field distribution. In the simulation process, frequency domain analysis was used to find the optimal capacitance value at the Larmor frequency. Lumped ports were used to provide quadrature excitation. For low-pass birdcage coil, capacitors were placed accordingly to the type of coil to determine the resonant frequency and the uniformity of the field it produces. Boundary conditions were assigned to the surface of the coil elements and the outer boundary of the solution domain enclosing the coil geometry. Scattering boundary conditions were also used to avoid any electromagnetic wave reflection back to the coil. The coil surface and the RF shield around the coil were assigned the perfect electric conductor (PEC) condition. Firstly, air domain was used to study the performance of the low-pass birdcage coil. The homogeneity was attained by quadrature excitation and optimal capacitance values of lumped elements in the coil.

COMSOL Multiphysics allows us to specify more than one frequency in order to observe the variation of any electromagnetic field parameter with respect to the frequency. For instance, the return loss  $S_{11}$  can be inspected by running simulations for a range of frequencies (frequency sweep) to see where smaller return loss is occurred within specified capacitance value. In order to obtain both homogenous and circularly rotating  $B_1$  field at the desired frequency, the capacitance was tuned by using the parametric sweep. The circularity of the field was evaluated by estimating the axial ratio of the magnetic field around the air phantom while the homogeneity of  $B_1$  field, was calculated using the standard deviation of the electric field around phantom.

In the frequency domain analysis, quadrature excitation was used to obtain homogeneous and circularly polarized magnetic field in the birdcage coil by tuning the capacitors properly. Quadrature excitation was driven from two ports which are equal in magnitude but with a phase of  $90^\circ$  to generate circularly polarized field inside the coil. Quadrature excitation generates circularly polarized field which is more homogeneous than linear excitation as a result of equal currents distribution along the legs of the coil. In addition, quadrature driven birdcage coil is more power efficient compared with linear drive, by reducing the RF power requirement by a factor of two.

$$B_{linear} = B_1 \cos(\omega t) x = (B_1^+) + (B_1^-) \quad (1)$$

where

$$B_1^\pm = \frac{B_1}{2} (\cos(\omega t)x \pm \sin(\omega t)y) \quad (2)$$

The first term represents a right-circularly polarized field while the second term represents left-circularly polarized field having equal magnitude of  $B_1/2$ .

## Simulating The Low-Pass Birdcage Coil with The RF Marker Prototype

For the air phantom, we were able to get excellent magnetic field homogeneity and  $B_1$  field circularity. However, it is necessary to check the alternation through the magnetic field homogeneity and  $B_1$  field circularity when the RF marker coil is placed into the low-pass RF birdcage coil in MRI. Therefore, we

applied the same analysis while the designed RF coil marker was placed at the center of the low-pass birdcage coil domain. First optimum capacitance value was observed for the altered domain at the Larmor frequency. Secondly the effect of designed RF marker was examined with respect to the RF field homogeneity and B<sub>1</sub> field circularity.

First of all, precise geometry of the experimental fabricated RF marker prototype was built in model by using drawing tools in Comsol Multiphysics. Both geometric parameters of sketched RF marker in Figure 3 and properties of materials defined in Comsol Multiphysics, completely identical with the RF marker prototype implemented in laboratory studies.

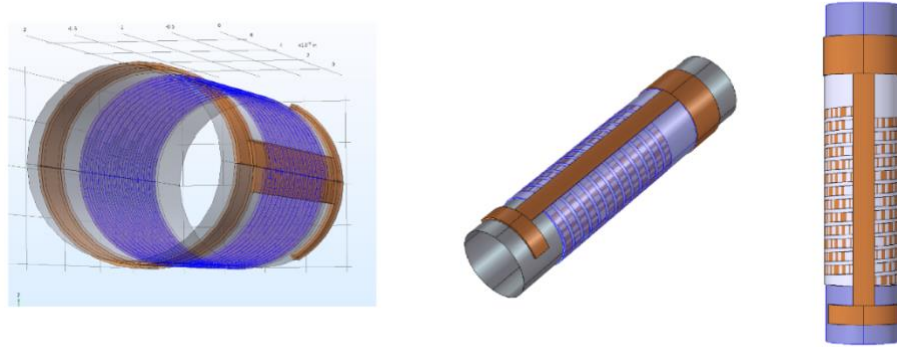


**Figure 3.** Dimensions of defined RF marker; radius: 1mm, number of turns of coil: 13, thickness of coil, capacitor plates and conductive layers: 30 μm, thickness of dielectric substance (Parylene C): 2.5 μm.

### Designs of RF Coils

**Helical Coil Design:** In this part of this study, different RF coil in RF marker designs were performed to evaluate their performance into the birdcage coil in MRI platform. Figure 4 indicates one helical coil that can be used as a coil in a RF marker, while Figure 5 indicates designed helical RF coil placed into ASTM phantom that simulates a saline water filled tank.

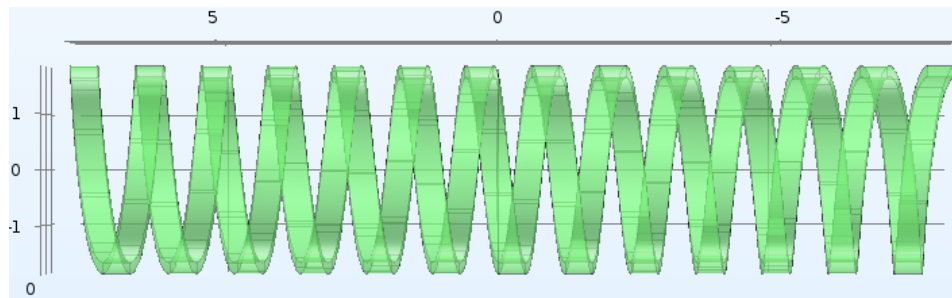


**Figure 4.** Designed helical RF coil image.

Geometric parameters of custom designed helical RF coil;

- Radius of the RF marker coil : 1.67 mm (length of 5 Fr catheter)
- Length of the RF marker coil : 5 mm
- Number of the turns of the RF marker coil : 13
- Pitch between the two coil turns (wp) : 100 μm
- Width of each coil turn (ww) : 200 μm

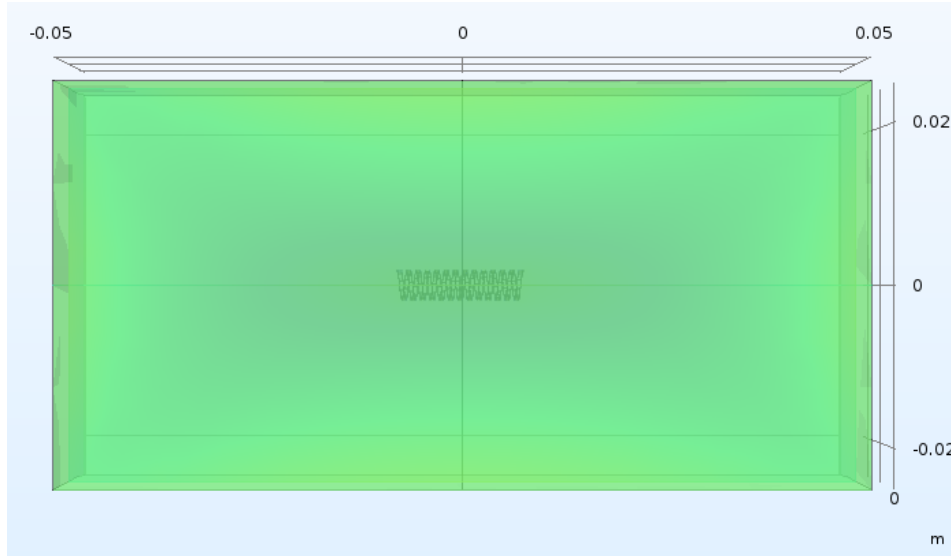


**Figure 5.** Image indicates designed helical RF coil placed into ASTM phantom that simulates a saline water filled tank with 5 cm width, 5 cm depth and 10 cm length.

**Double Helical Coil Design:** Figure 6 indicates double helical coil that can be used in a RF marker, while Figure 7 indicates designed double helical RF coil placed into ASTM phantom that simulates a saline water filled tank

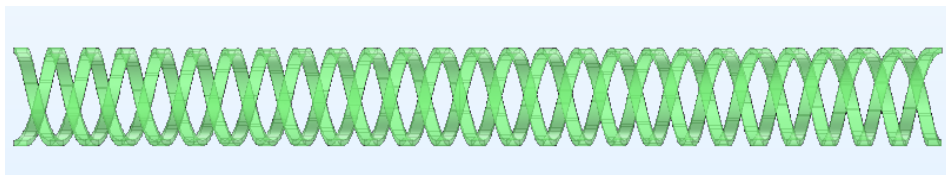


**Figure 6.** Image indicates designed double helical RF coils comprise 2 coils winded at the same direction but starting position of turns are different than each other.

Geometric parameters of custom designed double helical RF coil;

- Radius of the RF marker coil : 1.67 mm (length of 5 Fr catheter)
- Length of the RF marker coil : 3 cm
- Number of the turns of each coil : 13



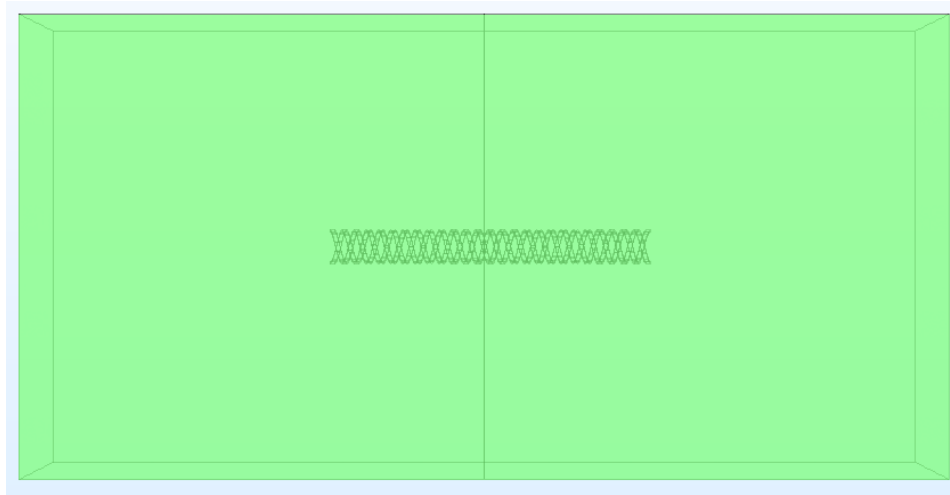


**Figure 7.** Image indicates designed double helical RF coil placed into ASTM phantom that simulates a saline water filled tank with 5 cm width, 5 cm depth and 10 cm length.

### 3. RESULTS & DISCUSSION

#### Simulating the Low-Pass Birdcage Coil without The RF Marker Prototype Capacitance Tuning Using Parametric Sweep

The designed birdcage coil has an inductor and many capacitors that have to resonate at the Larmor frequency of regarding MRI scanner. Initial tuning began by calculating the capacitance value, which is necessary for the coil to resonate at the desired frequency (63.8 MHz). Optimum capacitance value can be found by tuning the capacitor using a parametric sweep. The capacitance values range from 120 pF to 130 pF with a step capacitance of 0.5 pF were applied at 63.8 MHz, shown in Figure 8. The air phantom has a material property of electrical conductivity  $\sigma = 0$  S/m, relative permeability  $\mu_r = 1$  and relative permittivity  $\epsilon_r = 1$ .

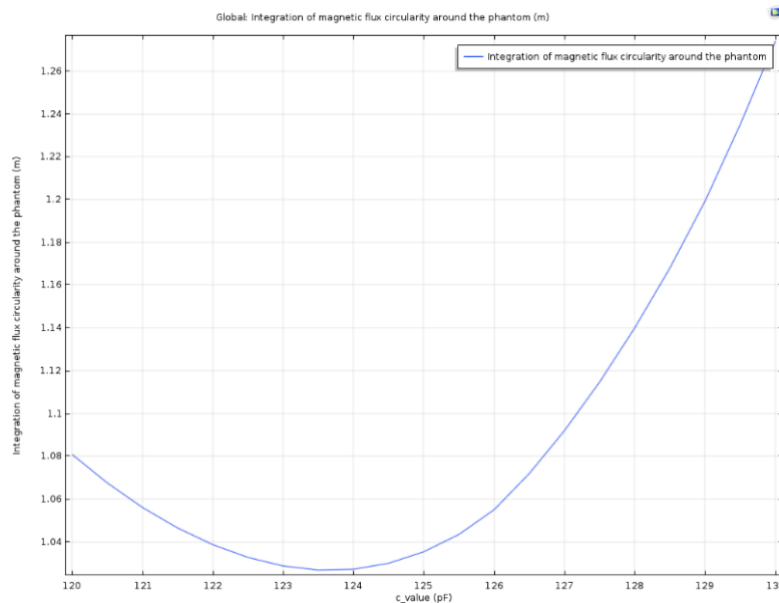


**Figure 8.** The axial ratio of the magnetic flux density for coil at 63.8 MHz (Larmor frequency of 1.5 Tesla MRI).



The circularity was evaluated by estimating the sum of the axial ratio of the magnetic field given as;

$$20 \log_{10}(B_{right} + B_{left}) / (B_{right} - B_{left}) \quad (3)$$

where  $B_{left}$  denotes the left-hand rotating component of magnetic flux while  $B_{right}$  denotes the right-hand rotating component of magnetic flux.

Respectively the homogeneity of the field is calculated using the standard deviation of the electric field. The optimal capacitance value for field homogeneity is the same as that for circularity. It can be observed the optimal value of the capacitance is close to 123.5 pF as indicated in Figure 8.

### Magnetic Field Homogeneity Evaluation of the Low-Pass Birdcage Coil

In order to evaluate the magnetic field homogeneity of the low-pass birdcage coil, a simulation was carried out for 8-leg low-pass birdcage coil loaded with air phantom as inspired studies mentioned before [4,5]. Capacitance value used on the rungs was 123.5 pF and the simulation frequency was 63.8 MHz. A homogenous magnetic field around the air phantom at 63.8 MHz was shown in Figure 9.

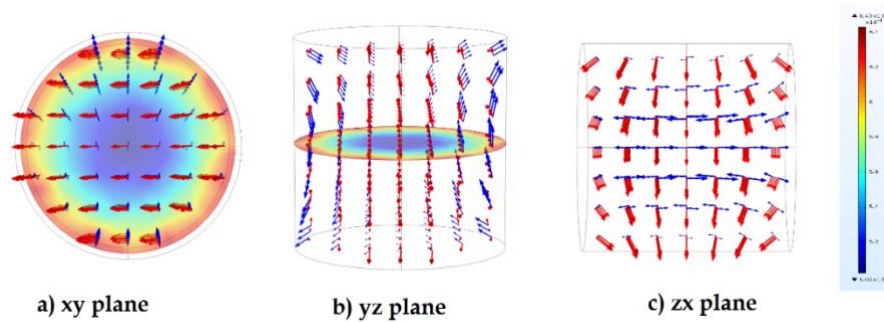


**Figure 9.** Magnetic flux density distribution with real (red) and imaginary (blue) part of the magnetic flux density for coil at 63.8 MHz. a) indicates xy plane, b) indicates yz plane, c) indicates zx plane [4,5].

### Simulating the Low-Pass Birdcage Coil with The RF Marker Prototype

#### Capacitance Tuning Using Parametric Sweep with The RF marker

Similar to the low-pass birdcage coil model without RF marker, optimum capacitance value was found by tuning the capacitor using a parametric sweep when designed RF marker was placed at the center of low-pass birdcage coil. The capacitance values range from 120 pF to 130 pF with a step capacitance of 0.5 pF were applied at 63.8 MHz as shown in Figure 10.

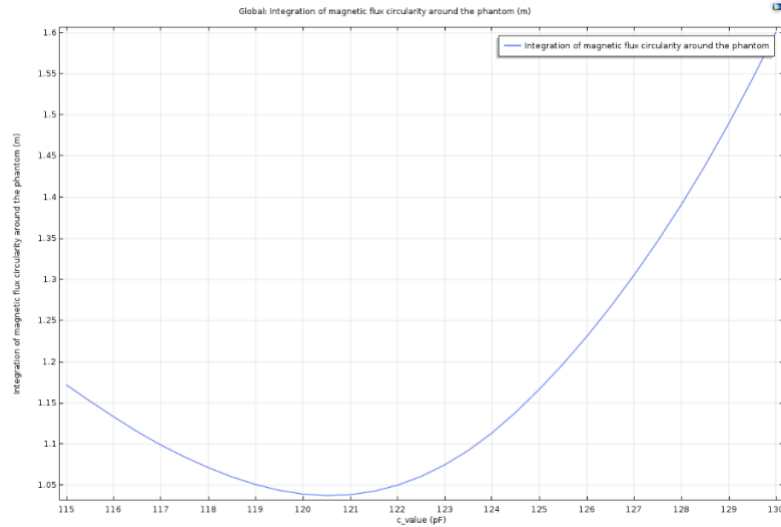


**Figure 10.** The axial ratio of the magnetic flux density for coil at 63.8 MHz (Larmor frequency of 1.5 Tesla MRI).

### Magnetic Field Homogeneity Evaluation of the Low-Pass Birdcage Coil with The RF Marker

In order to analyze the effect of RF marker on magnetic field homogeneity, the simulation was run for 8-leg low-pass birdcage coil loaded with air phantom and RF marker prototype. Capacitance value used on the rungs was 120.5 pF and the simulation frequency was 63.8 MHz. A homogenous magnetic field both around the air phantom and RF marker at 63.8 MHz was shown in Figure 11.

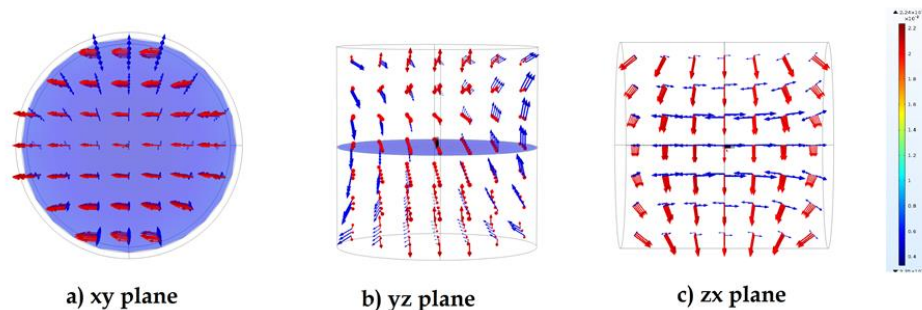


**Figure 11.** Magnetic flux density norm distribution with real (red) and imaginary (blue) part of the magnetic flux density for coil at 63.8 MHz. a) indicates xy plane, b) indicates yz plane, c) indicates zx plane.

As it is noticed in Figure 11, existence of designed RF marker in the low-pass birdcage coil domain didn't cause a significant distortion on both homogeneity and circularity of  $B_1$  field. However main reason for slightly alteration on the magnetic field homogeneity and circularity is RF marker induced additional non-uniform currents on the coil elements due to the different dielectric and permeability properties of the RF marker prototype.

### Electric Fields Norm Analysis of Helical RF Coils in Different Designs

After validation of custom-made birdcage coil into MRI environment, orientation depended performance analysis of RF coils were performed into the birdcage coil. For this aim, electric field norms of 2 different RF coils into different orientations according to the birdcage coil were evaluated. Helical coil designs were constructed into virtual platform that have similar geometric size with real RF marker prototypes fabricated in experimental studies.

## Electric Fields Norm Analysis of Single Helical RF Coil in Different Orientation

Electric fields norm of one helical RF coil into different orientations according to the birdcage coil were inspected as shown in Figure 12, in order to evaluate orientation dependency of the RF marker with respect to the standard MRI coils.

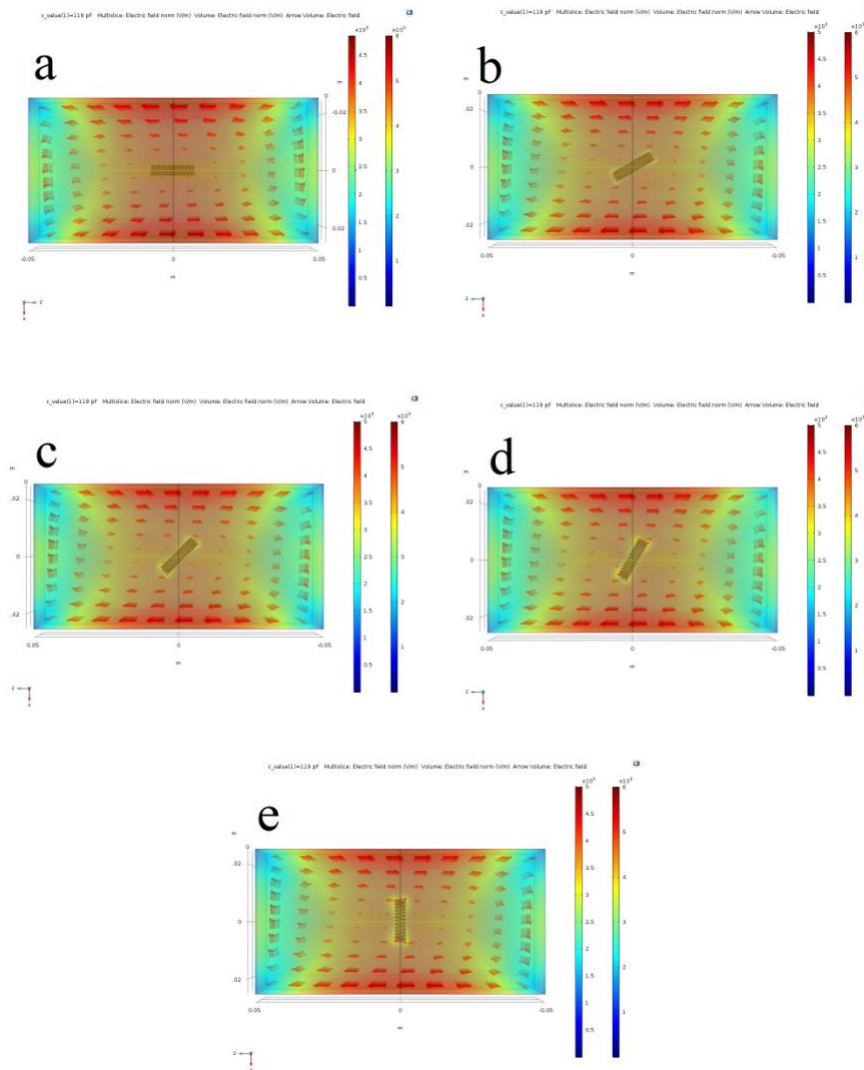


**Figure 12.** Image shows induced electric fields norm into the ASTM phantom and vicinity of the designed RF coil after the excitation of the birdcage coil at 63.8 MHz. Variation of electric field norms was observed when designed RF coil was a) parallel, b) 30° rotated, c) 45° rotated, d) 60° rotated, and e) perpendicular according to the birdcage coil. Red arrows show the direction of the electric field into volume of interest.

In Figure 12 the amount of electric field varies depending on the orientation of the RF coils. Electric field increases significantly with respect to the increase in rotation angle between the RF coil and the birdcage coil. The highest induced electric field is observed when the RF coil is placed perpendicular to the birdcage coil as it is expected in Maxwell's equations.

Similarly, with the excitation by the birdcage coil, electric field norms at the surface of the RF coil were examined in Figure 13. The most induced electric field was seen when the RF coil is oriented perpendicular to the birdcage coil.

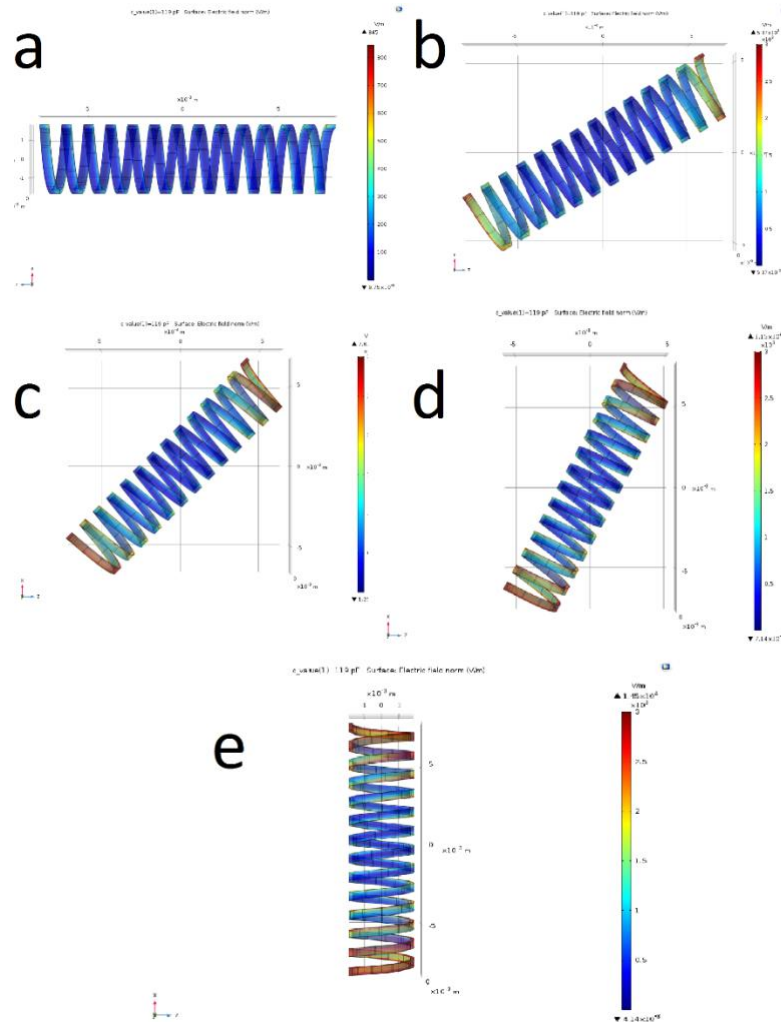


**Figure 13.** Image shows induced electric field norms at the surface of the RF coil after the excitation by the birdcage coil. Electric field norms was observed when the designed RF coil was a) parallel, b) 30<sup>o</sup> rotated, c) 45<sup>o</sup> rotated, d) 60<sup>o</sup> rotated, and e) perpendicular according to the birdcage coil.

### Electric Field Norm Analysis of Double Helical RF Coil in Different Orientation

Another orientation depended performance analysis of RF coil were performed into the birdcage coil by using a different geometric design. Electric fields norm of two helical RF coil into different orientations according to the birdcage coil were observed in Figure 14, in order to evaluate orientation dependency of RF markers with respect to the standard MRI coils.

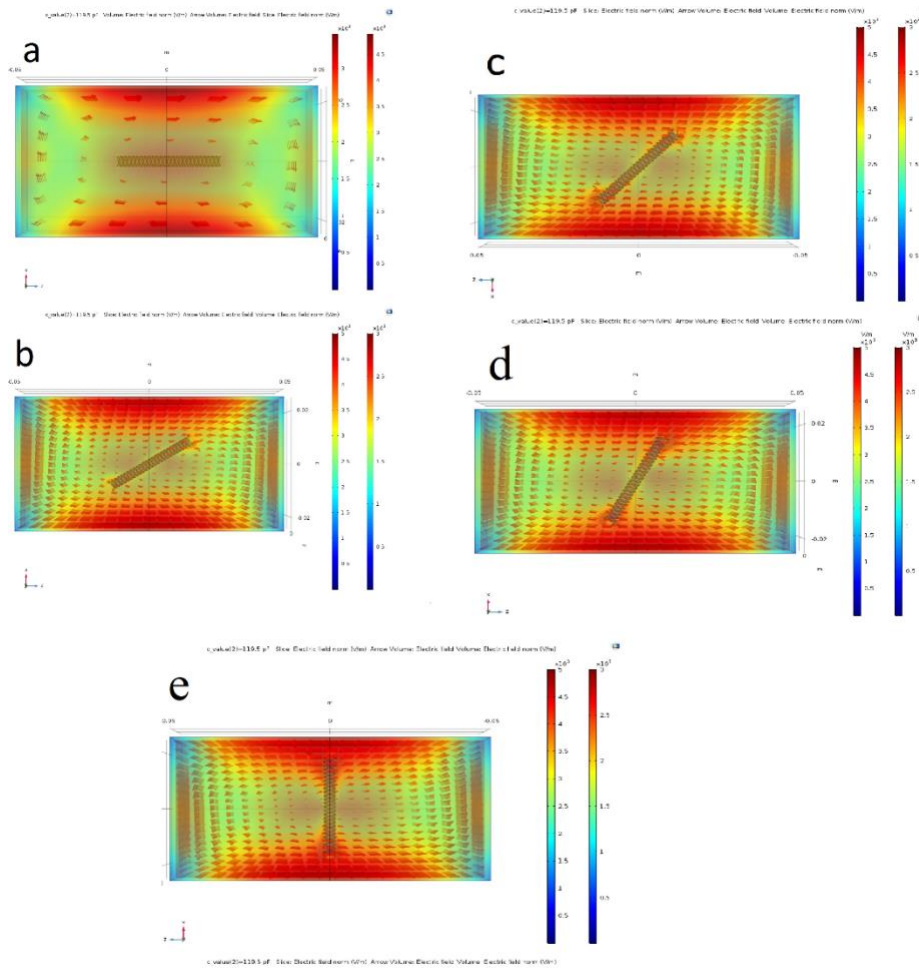


**Figure 14.** Image shows induced electric field norms into the ASTM phantom and vicinity of the designed double RF coil after the excitation of the birdcage coil at 63.8 MHz. Variation of electric field norms was observed when designed double RF coil was a) parallel, b) 30° rotated, c) 45° rotated, d) 60° rotated, and e) perpendicular according to the birdcage coil. Red arrows show the direction of the electric field into volume of interest.

Like single RF coil design, the amount of electric field varies depending on the orientation of the RF coils. Electric field increases significantly with respect to the increase in rotation angle between the double RF coil and the birdcage coil. The highest induced electric field is observed when the double RF coil is placed perpendicular to the birdcage coil as it is expected in Maxwell’s equations.

Similarly, with the excitation by the birdcage coil, electric field norms at the surface of the double RF coil were examined in Figure 15. The most induced electric field was seen when the double RF coil is oriented perpendicular to the birdcage coil.

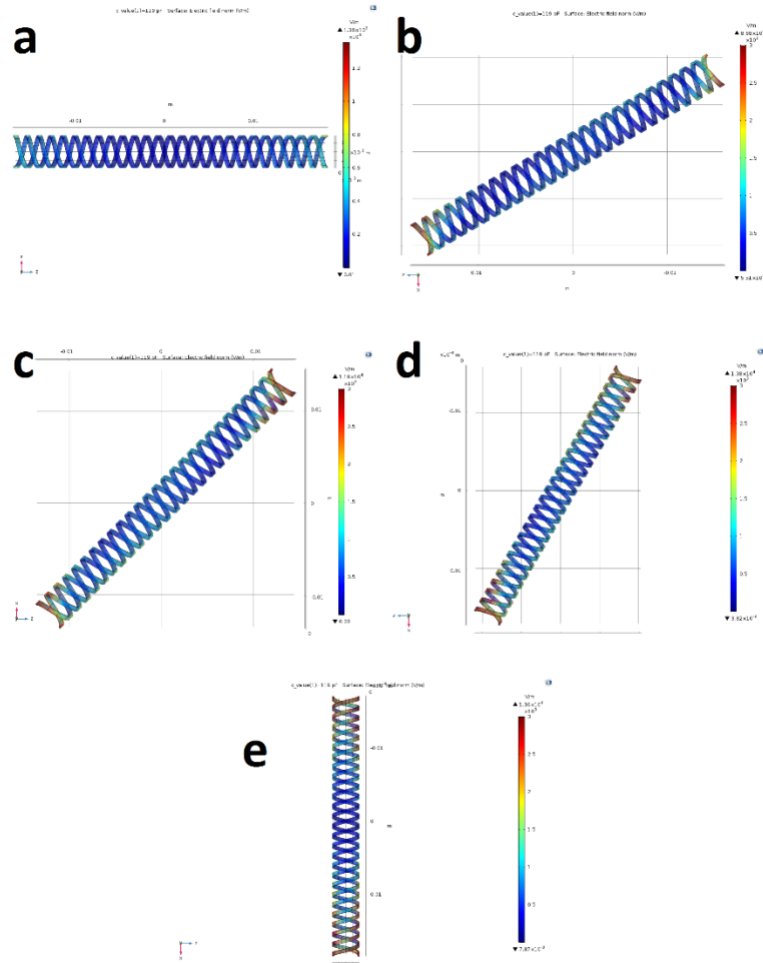


**Figure 15.** Image shows induced electric field norms at the surface of the double RF coil after the excitation by the birdcage coil. Electric fields norm was observed when the designed double RF coil was a) parallel, b) 30° rotated, c) 45° rotated, d) 60° rotated, and e) perpendicular according to the birdcage coil.

In conclusion, the results of simulations are consistent with former experimental works and results in the literature [1]. Although there are some difficulties at examining the interactions between micro size instruments and huge size environments such as micro coils and MRI platform, it is clear that the FEM simulations will be a reliable test and evaluation method in order to examine magnetic and electrical characteristics of designed RF coils and so RF markers.

#### 4. CONCLUSION

In this study, 3D FEM modeling of manufactured RF marker prototype into a birdcage coil was figured out by using COMSOL Multiphysics software program. After ensuring the validation of performed MRI platform with compliance with ASTM phantom results, affectivity of the birdcage coil and MRI environment for 1.5 Tesla was examined with capacitance tuning. After obtaining optimum capacitance value, homogeneity of magnetic field was analyzed when the RF marker prototype was placed into center of the birdcage coil. Moreover, performances of 2 different RF coil designs were evaluated while coil designs were positioned into different orientation angles with respect to the birdcage coil.

Capability of the modeling the interactions between a RF marker and a birdcage coil into a MRI environment experienced in this study, will lead many new simulation designs including comparison of



different forms of RF markers, coil orientations and their characteristics. Accordingly, it is possible to construct custom made novel coil designs that can be used as a RF marker and as a standard MRI coil.

By providing these simulation models will be very beneficial for saving time to foresee the optimum coil parameters and RF marker performances without fabrication and real MRI experiments.

## 5. REFERENCES

1. Baysoy, E., Yildirim, D., Ozsoy, C., Mutlu, S., Kocaturk, O. (2016). Thin fillm based semi-active resonant marker design for low profile interventional cardiovascular MRI devices. *Magnetic Resonance Materials in Physics, Biology and Medicine*, 30(1), 93-101. Doi:10.1007/s10334-016-0586-8).
2. Lederman, R.J. (2006). NIH Public Access, 112(19), 3009-3017.
3. Barkhausen, J., Kahn, T., Krombach, G.A., Kuhl, C.K., Lotz, J., Maintz, D., Ricke, J., Schönberg, S.O., Vogl, T.J. and Wacker, F.K. (2017). White Paper: Interventional MRI: Current Status and Potential for Development Considering Economic Perspectives, Part 1: General Application. *RoFo: Fortschritte auf dem Gebiete der Rontgenstrahlen und der Nuklearmedizin*, 189(7), 611-623. Doi:10.1055/s-0043-110011.
4. Gurler, N. & Ider, Y.Z. (2015). Numerical methods and software tools for simulation, design, and resonant mode analysis of radio frequency birdcage coils used in MRI. *Concepts Magn. Reson.*, 45, 13-32. Doi:10.1002/cmr.b.21279.
5. Tadesse, Y. (2015). The electromagnetic simulation of birdcage coils for MRI based on Finite element method. Master of degree thesis, Youngstown State University, Ohio, The United States of America.
6. Sonmez, M., Saikus, C.E., Bell, J.A., Franson, D.N., Halabi, M., Faranesh, A.Z., Ozturk, C., Lederman, R.J., Kocaturk, O. (2012). MRI active guidewire with an embedded temperature probe and providing a distinct tip signal to enhance clinical safety. *Journal of Cardiovascular Magnetic Resonance*, 14, 38. Doi:10.1186/1532-429X-14-38.